P2.26 Orographic Effects on a Conditionally Unstable Flow over an Idealized Three-Dimensional Mesoscale Mountain

S. H. Chen*
University of California, Davis, CA
Y.-L. Lin
North Carolina State University, Raleigh, NC

1. Introduction

In studying conditionally unstable flow over an idealized two-dimensional mesoscale mountain, Chu and Lin (2000) identified three moist flow regimes, which are controlled by the moist Froude number defined as $V / N_w h$. In this paper, we make idealized numerical experiments to help identify the 3D moist, rotational flow regimes and understand the dynamics. In additional to the moist Froude number (F_w), we will also investigate effects of CAPE on moist flow regimes. Many heavy orographic rain events occurred over the Alps started near the Lago Maggiore region, which are near the concave region of the southern side of the Alpine mountains and under the southerly or southeasterly low-level flow. In this study, we will use a basic flow with uniform speed and moisture distribution to investigate whether a convergence can be produced near the concave region or not.

2. Model Description and Experiment Design

The Weather Research and Forecast (WRF) model (Klemp et al. 2001) is adopted for this study. Detailed information about this model may be found in the website: www.wrf-model.org. The incoming flow is assumed to be homogeneous. The surface potential temperature is 300 K with a dry Brunt-Vaisala frequency of 0.0123 s^{-1}. The relative humidity decreases from 93% at sea level to 25% at 12 km height, and then it stays constant of 25% to model top. The numerical experiments are summarized in Table 1.The ridge-like orography has an east-west length of 700 km, and a north-south width of 400 km, which decreases from the ridgeline by a square cosine function. The parameters h, a (half width), and Δx (= Δy) used in the numerical experiments are 2 km, 100 km, and 30 km. The vertical grid interval is stretched from 30 m at the lowest level to 500 m near the domain top. The domain grid points are 111×111×58 in *x*-*y*-*z* direction. A 5-km sponge layer is imposed on top of the physical domain (25 km) to absorb waves. The time interval is 60 s, and the nondimensional integration time (tV/a) is set to be 4.32.

3. Moist Flow Regimes and Dynamics

The early response of a dry airflow on an f-plane (Case 1) to a ridge-like mountain is similar to that of non-rotating flow. At 8 h (Fig. 1a), the upstream flow has a significant left turning and the high pressure region is shifted toward left side of the mountain with the maximum pressure perturbation located over the upslope. The flow turns anticyclonically over the mountain ridge and then resumes its original direction at a distance about the north-south mountain scale. A region of strong low pressure perturbation is located to the east side of the lee slope and immediately downstream region. The vertical velocity field at z=1 km (Fig. 1b) shows an upward (downward) motion over upslope (downslope). To the north side of the downward motion over the lee slope, a region of strong upward motion is produced, which is associated with the hydraulic jump (Fig. 1c). In general, the dry flow response is similar to that simulated by Schneidereit and Schar (2000).

a. Moist flow regimes

Fig. 2 shows the accumulated precipitation and surface streamlines at $tV/a = 4.32$ for Case 2 ($F_w = .666$; $V = 15$ ms^{-1}). The precipitation area is arc-shaped and wraps around the mountain with the arms extending to the northwest side of the mountain (Fig. 2a) and the rainfall region spreads over both upstream and downslope of the mountain range. The maximum upstream rainfall is located over the upslope and is more than 50 mm at $tV/a = 4.32$ (t=8 h). The upstream convective system propagates upstream slowly (Figs. 2a and 2b). This flow possesses characteristics of regimes I and II, i.e. regime I-II. *Regime II* is defined as a *regime with quasi-stationary upslope and downslope convective systems*.

Opposite to the dry case (Fig. 1a), the upstream flow turns to the right slightly ahead (to the south) of the upstream convective system and then a strong southeasterly jet over the upslope and behind (to the north) of the upstream convective system, as depicted by the streamlines for a moist flow (Fig. 2b). In a rotating flow, the center line is shifted to the eastern edge of the mountain (Figs. 1a and 1b). Similar to the dry flow (Fig. 1a), the low pressure downstream is located to the northeast of the mountain ridge, but occupies a much larger area than that upstream and that produced in dry flow. The overall flow passing over the mountain and convective systems is still anticyclonic. A density current is produced over the upslope by the convective system (Fig. 2c). Ahead of the density current there exists a strong convective system, which is propagating upstream slowly. In addition to the major convective system over the upslope, there exists a weaker convective system located over the lee slope, which appears to be generated by the

* Corresponding author address: Dr. Shu-Hua Chen, shachen@ucdavis.edu.

hydraulic jump. A strong downslope wind is blowing down the lee slope.

Figure 3a shows the accumulated precipitation, wind vector field and a N-S vertical cross section of x=0 at $tV/a = 4.32$ for Case 3 ($F_w = .333$; $V = 7.5$ ms^{-1}). The upstream portion of the rainfall area has extended to about 500 km with the maximum rainfall of over 60 mm. A small-scale cyclonic (anticyclonic) vortex forms to the northeast (northwest) of the mountain. The western branch of the flow also recirculates back to the lee slope. The maximum upward motion is located over the upslope (Fig. 3b). In the beginning, the convection is generated over the upslope, which is then propagating upstream associated with the density current (Fig. 3c). The flow splitting can also be seen from the streamline field (Fig. 1b), while the mountain blocks a significant amount of flow upstream. This flow may be characterized as a *regime with upstream-propagating convective system (Regime I).*

When F_w increases further to 1.332 ($V = 30\, ms^{-1}$; Case 4), the flow behaves very differently. The dimensional time is 4 h. First, there is no apparent horizontal deflection of the basic flow except near the west and east edges of the mountain (Fig. 4a). The lee side low is produced by adiabatic warming associated with the downslope wind. The lack of upstream turning is caused by a negligible role played by the Coriolis force. Second, a strong convective system, which is produced by the hydraulic jump, forms over the lee slope and propagates downstream (Figs. 4a and 4c). This flow may be characterized as a *regime with quasi-stationary upslope convective system and downstream-propagating convective system (Regime III).*

b. Effects of mountain geometry

In Case 2B, we add a western flank, similar to that in Schneidereit and Schar (2000) but with a uniform southerly wind, to the ridgelike mountain of Case 2. Fig. 5a shows the total rainfall at $tV/a = 4.32$. The rainfall is concentrated along the southern slopes of both the east-west ridge and the western leg. The maximum accumulated rainfall over 8 h is over 60 mm, which is comparable to Case 2. Note that the maximum rainfall is not located at the concave region. The flow near the concave region has a very strong eastward component, which helps produce the strong upward motion near the concave region (Fig. 5b). This upward motion is produced by the convergence of the southeasterly jet over the upslope and foothill of the east-west ridge and the deflected southerly wind near the foothill of the western leg. The Coriolis force helps make the leftward (westward) turning of the flow near the southern slope and produce strong upward motion over the upslope near the concave region. The flow behavior is similar to that simulated by Schneidereit and Schar (2000) and Rotunno and Ferretti (2001). That is, there exist two types of flow, one going around the east-west ridge and the other going over the western flank.

c. Sensitivity to CAPE

Fig. 6 shows the flow response to a flow with CAPE=1000 $J\ kg^{-1}$. In general, the flow response is similar to Case 2 except the upstream convective system and rainfall are confined at the foothill and upslope (Figs. 6a and c). Thus, the flow belongs to Regime II, i.e. flow with quasi-stationary upslope and downslope convective systems. By comparing with Case 2 (CAPE=1900 $J\ kg^{-1}$), we may conclude that a flow tends to shift to lower regime when CAPE increases.

4. Application to MAP IOP-2B and IOP-8

One of the major differences between MAP IOP-2B and IOP-8 is the precipitation pattern. In IOP-2B, the rainfall was concentrated over the upslope and slightly upstream of the foothill, while the rainfall in IOP-8 was extended further upstream. Based on the soundings obtained at Milan at 00UTC 20 September for IOP-2B and 00UTC 21 October for IOP-8, the F_w were roughly estimated to be 0.35 and 0.18 for IOP-2B and IOP-8, respectively. Therefore, both IOP-2B and IOP-8 belong to Regime I, although IOP-8 has a much smaller F_w. This also helps explain why the rainfall associated with IOP-8 extended further upstream compared with that with IOP-2B.

5. Concluding Remarks

In this study, we have found:

(1) Three flow regimes are identified for a conditionally unstable flow over a three-dimensional mountain: (I) regime with upstream-propagating convective system, (II) regime with quasi-stationary upslope and downslope convective systems, and (III) regime with quasi-stationary upslope convective system and downstream propagating convective system.

(2) In addition to the mechanisms of localized LLJ and inhomogeneous moisture distribution, the convergence and upward motion near a concave region may be produced by the Coriolis force and latent heating.

(3) When CAPE increases, the flow tends to shift to lower regime.

(4) Estimates of F_w for IOP-2B and IOP-8 from Milan soundings imply that both of them belong to Regime I, although F_w is much smaller for IOP-8. This helps explain the farther upstream extension of rainfall pattern for IOP-8.

Acknowledgments: This work is supported by US NSF Grant ATM-0096876 and Air Force Weather Agency.

References

Chu, C.-M., and Y.-L. Lin, 2000: Effects of orography on the generation and propagation of mesoscale convective systems in a two-dimensional conditionally unstable flow. J. Atmos. Sci. , **57**, 3817-3837.

Klemp, J. B., and W. C. Skamarock, and J. Dudhia, 2001: Prototypes for the WRF (Weather Research and Forecast] model. 9th Conf. Meso. Processes, AMS (also see www.wrf-model.org)

Lin, Y.-L, J. A. Thurman, and S. Chiao, 2001: Influence of synoptic and mesoscale environments on heavy orographic rainfall associated with MAP IOP-2B and IOP-8. MAP Newletter, **15**.

Rotunno, R. and R. Ferretti, 2001: Mechanisms of intense Alpine rainfall. J. Atmos. Sci., 58, 1732-1749.

Schneidereit, M., and C. Schar, 2000: Indealised numerical experiments of Alpine flow regimes and southside precipitation events. Meteor. Atmos. Phys., **72**, 233-250.

Table 1. Characteristics of the Numerical Experiments

Case	V	F_w	Integration Time (h)	Moist Flow Regime	Upstream/upslope/downstream convective systems	Special Characteristics
1	15.0	NA	8	NA	NA	Dry, F_d=0.600
2	15.0	0.666	8	I-II	Yes/yes/no	
3	7.5	0.333	16	I	Yes/no/no	
4	30.0	1.332	4	III	No/yes/yes	
2A	15.0	0.666	8	I-II	No/yes/no	f=0
2B	15.0	0.666	8	I-II	Yes/yes/no	Arc-shaped mountain
2C	15.0	0.661	8	II	No/yes/no	CAPE=1000 J/kg

* $h = 2\ km$, $a = 100$ km, $N_w = .01127\ s^{-1}$, $f = .0001\ s^{-1}$ and CAPE = 1900 $J\ kg^{-1}$ for all cases except cases 1 and 2C.

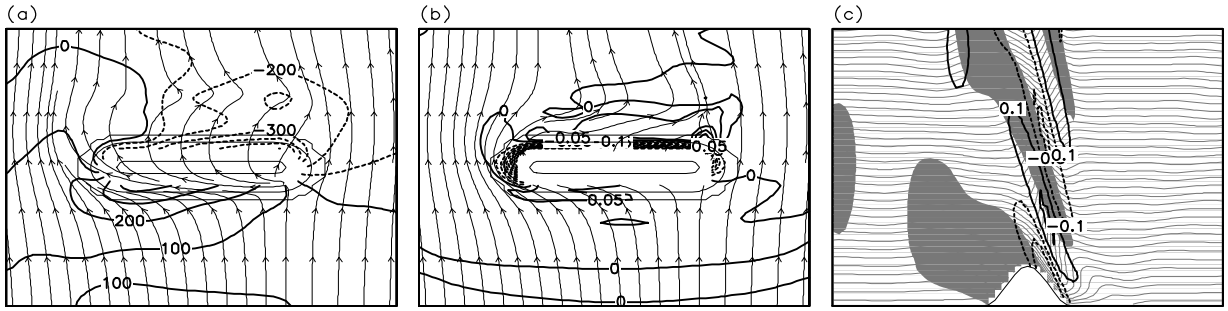

Fig. 1: (Case 1) Dry airflow over a ridge-like mountain. (a) The pressure perturbation and streamlines 30 m above the surface, (2) w (ms^{-1}) (thick lines) and streamlines at z=1000 m, and (c) w (ms^{-1}) (thick lines) along x=-60 km and q (thin lines) after 8-h (Vt/a=4.32) simulation. The topography is plotted in (a) and (b) with thin solid lines. The plotting domain is (1800, 1800, 14km).

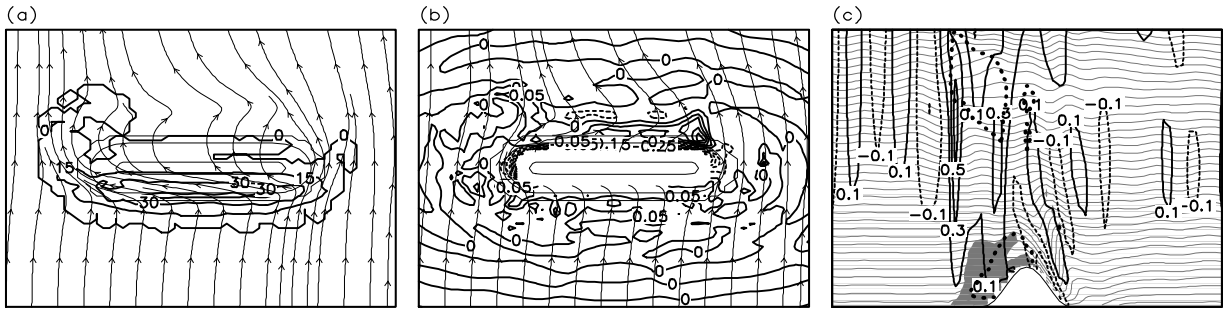

Fig. 2: (Case 2 – Regime I-II) Rotating moist flow over a ridge-like mountain. (a) The surface streamlines and accumulated precipitation (mm) (thick lines), (2) w (ms^{-1}) (thick lines) and streamlines at z=1000 m, and (c) w (ms^{-1}) (thick lines) along x=0 km and q (thin lines) after 8-h (Vt/a=4.32) simulation. In (c), the thick dotted line denotes the total water content of 0.1 $g\ kg^{-1}$ and $\theta' < 0.5$ K is shaded. The plotting domain is (1800, 1800, 14km).

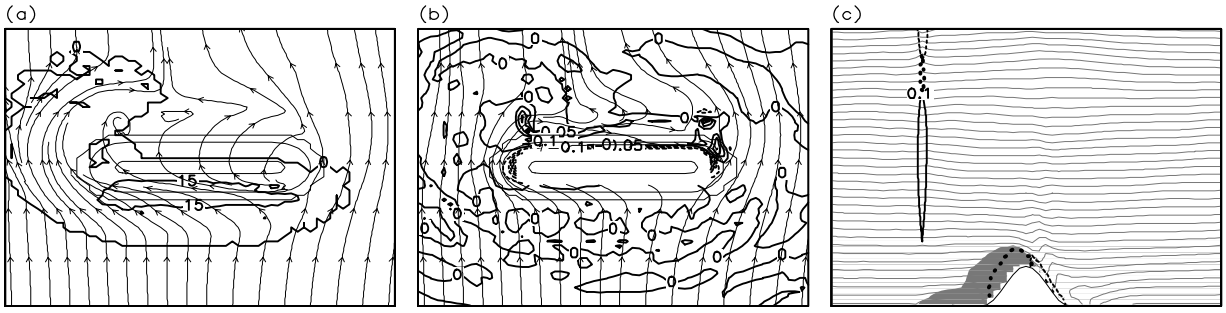

Fig. 3: (Case 3 – Regime I) Same as Fig. 2 except for $F_w = 0.333\,(V = 7.5\,ms^{-1})$.

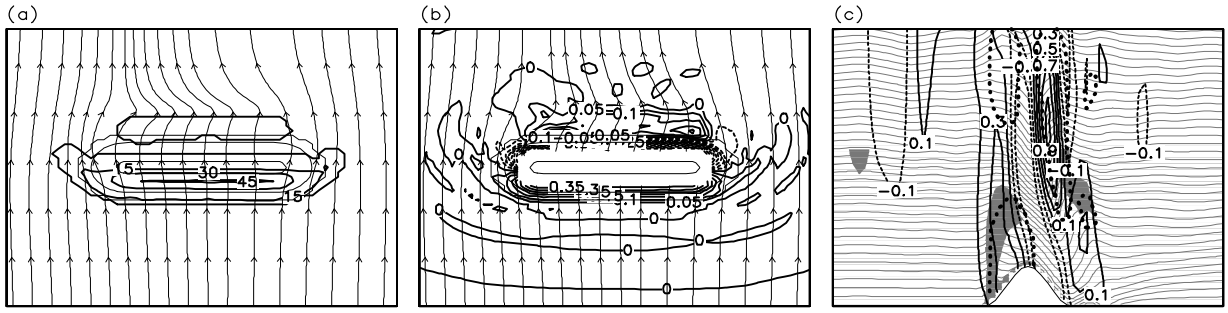

Fig. 4: (Case 4 – Regime III) Same as Fig. 2 except for $F_w = 1.332\,(V = 30\,ms^{-1})$.

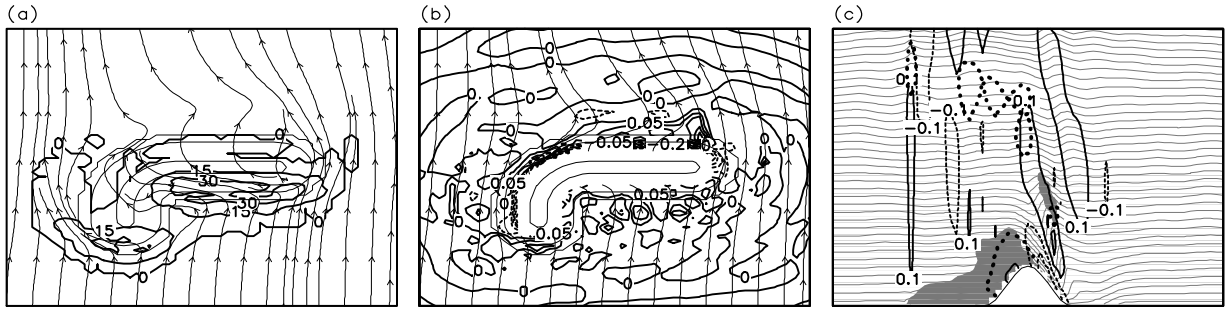

Fig. 5 (Case 2B): Same as Fig. 2, except with an arc-shaped mountain and panel c is along x=-60 km.

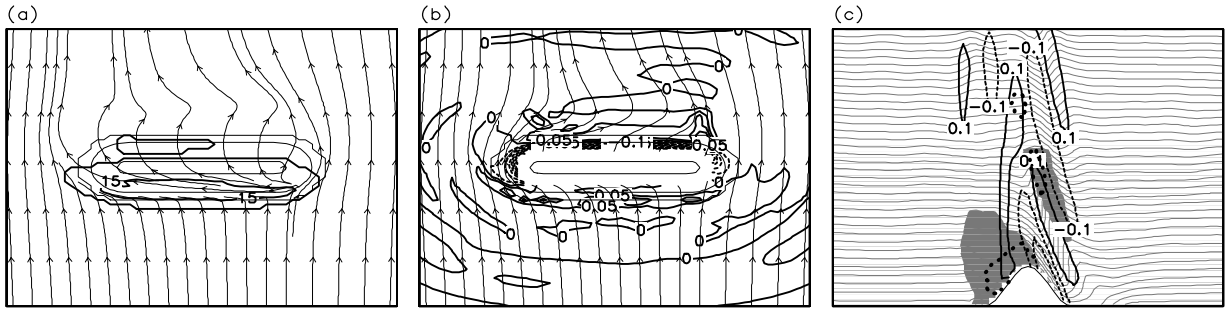

Fig. 6 (Case 2C): Same as Fig. 2, except with CAPE=1000 $J\,kg^{-1}$.